

PACS numbers: 87.19.xj; 87.57.Q–; 87.64.kp; 87.64.kv
DOI: 10.1070/QE2014v044n08ABEH015545

Multimodal diagnosis and visualisation of oncologic pathologies

V.P. Zakharov, I.A. Bratchenko, O.O. Myakinin, D.N. Artemyev,
D.V. Kornilin, S.V. Kozlov, A.A. Moryatov

Abstract. **The combined application of optical coherence tomography, Raman and autofluorescence spectroscopy of biotissues for the analysis of human malignant neoplasms is demonstrated. Rapid investigation of vast biotissue regions (at the scale of entire organs) is possible using the autofluorescence response. After selection of possible zones of pathologies one can visualise the neoplasm topology in the zone of interest with micron precision by using optical coherence tomography. In the case of suspecting the malignancy the analysis of the biotissue Raman spectrum is carried out that allows identification of the neoplasm type with the sensitivity and specificity ~85%. An experimental scheme is proposed with the combined use of the abovementioned methods, which is a prototype of the medical system for complex analysis of neoplasms.**

Keywords: *multimodal diagnosis, noninvasive diagnosis, optical coherence tomography, Raman scattering, autofluorescence analysis.*

1. Introduction

The number of annually registered malignant neoplasms grows, and, according to the prognosis of medical specialists, the number of oncological patients will steadily increase in nearest decades [1]. During the last 20–25 years the number of registered malignant and benign neoplasms of skin, lungs, intestine and other internals has increased by several times [2, 3]. The efficiency of diagnosis of malignant neoplasms is different for different types of cancer, but generally stays insufficient at the stage of early diagnosis by general practitioners, which is due to the complexity of interpretation of clinical differential indicators of the neoplasms at the early stage [4]. The low efficiency of early diagnosis of oncological diseases favours the development of neoplasms and, finally, increases the risks of fatal outcome. In this connection, the use of instrumental diagnostic methods is necessary.

The method of optical coherence tomography (OCT) allows the investigation of tumour structure [5, 6]. In contrast to such methods as ultrasound examination, computer tomography and magnetic resonance tomography, which can be useful for the determination of the tumour invasion region, OCT allows detection of biotissue inhomogeneity with the size of a few microns. OCT is used for 2D and 3D imaging of eye, breast, lungs, skin, large intestine, larynx and other tissues. In particular, it was shown that OCT is a powerful tool for the diagnosis of basal cell carcinoma (basalioma) [7] in relation with its specific spatial localisation. Nevertheless, in most cases the OCT yields only detailed information about the morphological features of the tumour and does not allow precise determination of the cancer type. As a rule, the sensitivity and specificity of diagnosis using the OCT method does not exceed 75%–85% for different types of cancer. Moreover, in many cases the high sensitivity (about 85%) is accompanied by low specificity (60%–70%). It follows that the OCT method should be combined with other spectral methods to provide precise identification of the tumour type.

One of such methods of neoplasm noninvasive analysis is Raman scattering (RS) spectroscopy. This method was used by many authors to analyse neoplasms in the *in vivo* and *ex vivo* studies of skin [8], lungs [9], breast [10], intestine [11] and other biotissues. Thus, in Refs [12, 13] the high efficiency of RS method was demonstrated in the diagnosis of melanoma and squamous cell carcinoma of skin. The sensitivity of 91% and the specificity of 75% were attained. However, in mass screening studies the sensitivity and specificity of the method is essentially lower [14]. This fact is related to the strong dependence of the intensity of RS peaks upon the concentration of the tissue biochemical components and to the exploitation of absolute criteria in the methods, proposed in the abovementioned papers. In this connection, it is an urgent problem to develop the methods of variant RS analysis for diagnosis of neoplasms in humans, as well to use other methods of spectral analysis for increasing the precision of such diagnosis.

One of the promising methods for spectral analysis of biotissues is the study of their autofluorescence (AF). This approach allows one to compare the spectral characteristics of a neoplasm and the adjacent healthy tissue, which, in turn, enhances the informativity of spectral studies.

Thus, in order to visualise tumours it is reasonable to use the OCT method, and for increasing the precision of the investigations we propose here to use the phase method of determining the type of neoplasm, together with the Raman spectroscopy method. We consider different mathematical approaches to classifying the groups of neoplasms. It is also proposed to use the AF of the biotissue for rapid determination of the neoplasm boundaries and increasing the precision of diagnosis.

V.P. Zakharov, I.A. Bratchenko, O.O. Myakinin, D.N. Artemyev, D.V. Kornilin S.P. Korolev Samara State Aerospace University (National Research University), Moskovskoye shosse 34, 443086 Samara, Russia; e-mail: zakharov @ssau.ru;
S.V. Kozlov, A.A. Moryatov Samara State Medical University, ul. Chapayevskaya 89, 443086 Samara, Russia

Received 16 April 2014; revision received 15 June 2014
Kvantovaya Elektronika **44** (8) 726–731 (2014)
Translated by V.L. Derbov

2. Materials and methods of study

2.1. Experimental setup

For *ex vivo* and *in vitro* experiments we used the laboratory setup, combining the principles of OCT and RS (Fig. 1). The setup included a thermally stabilised LML-785.0RB-04 semiconductor laser unit (*8*) (the centre radiation wavelength λ = 785±0.1 nm, the power up to 150 mW) for exciting RS, a broadband laser diode (*1*) (λ = 840±25 nm, 20 mW), a Michelson interferometer (*2*), a spectrograph (*5*) with a digital CCD camera (*6*). The digitisation of the interference pattern was implemented using the image capture card. When recording A scans by means of the OCT technology, the image registration was carried out with the limiting resolution of 3.7 μm. The selection of RS spectral lines was implemented using a band-pass filter. Then, by means of a dichroic mirror the backscattered laser light, the AF and RS signals were directed onto the broad-band filter that did not transmit the probe radiation. The RS and fluorescence spectra were recorded using the Sharmrock SR-303i spectrograph and the digital iDus camera with the resolution of 0.05 nm and low level of noise. The final RS spectrum was obtained after elimination of the AF component from the registered signal.

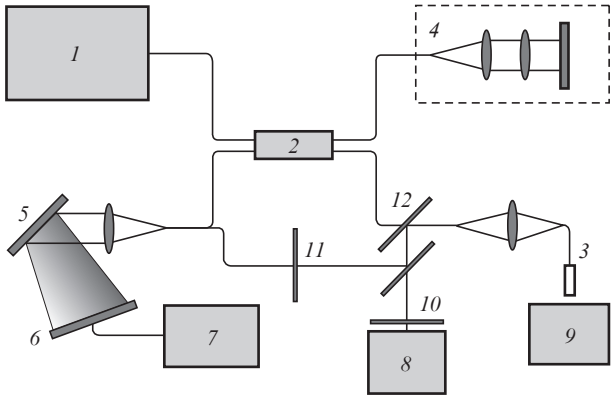

Figure 1. Scheme of the experimental setup:
(*1*) broadband light source ($\lambda \sim$ 840 nm); (*2*) Michelson interferometer; (*3*) optical fibre probe; (*4*) reference arm of the OCT interferometer; (*5*) spectrograph with high-sensitivity CCD camera (*6*); (*7*) computer; (*8*) semiconductor laser (λ = 785 nm); (*9*) sample under study; (*10*) band-pass filter; (*11*) broadband filter; (*12*) dichroic mirror.

2.2. Object of study

As an object of *ex vivo* studies we used samples of various neoplasms of human skin and lungs, removed in surgical departments of Samara Regional Clinical Oncology Dispensary. In the series of *ex vivo* experiments the RS spectra of 23 neoplasms were recorded, among which there were 8 melanomas, 4 samples of basalioma, 6 samples of pigmented nevus, and 5 other benign neoplasms, as well as the RS spectra of 10 samples of normal skin. In the *in vivo* experiments 46 RS spectra were analysed that were obtained in the study of 9 melanomas, 8 basaliomas, 2 nevuses, 2 benign tumours, and 25 samples of healthy skin. In the *ex vivo* studies of lung neoplasms the objects were 11 samples of adenocarcinoma and 11 samples of squamous cell carcinoma; for each of the samples the signal from healthy tissue was also recorded. The samples with the characteristic size 2–4 cm in each of three dimensions represented a region of pathology surrounded by healthy tissue.

The registration of OCT images and RS spectra was implemented using the system, presented in Fig. 1. The face of the optical fibre probe (*3*) was placed above the studied region at the distance 5–7 mm. Positioning at the object of study for recording OCT images, implemented using a galvanic drive with a system of mirrors, allowed us to match the OCT and RS data. After the OCT image recording and determination of healthy and pathological tissue zones, a series of RS spectra was obtained from the region of neoplasm and from the healthy skin. The investigation time for one patient did not exceed 3–5 min. The obtained data were analysed by comparison with the results of histological study.

All volunteers that took part in the experiments were more than 18 years old. Their preliminary investigation and preparation to surgical treatment were carried out at Samara Regional Clinical Oncology Dispensary. The study was positively evaluated by the Bioethic Committee of the Samara State Medical University.

3. Results of biotissue studies

3.1. OCT method for biotissue imaging

As was already mentioned in the Introduction, OCT offers an opportunity to determine the type of some of the oncological pathologies. Figure 2 presents the OCT images (B scans) of basal cell carcinoma and malignant skin melanoma. High resolution of the OCT makes it possible to discern the smallest details in the region of the pathology growth and to determine the invasion zone precisely. However, practically it is rather difficult to determine the type of particular tumour using the OCT method solely. While for the basal cell carcinoma the roundish shape of the 'nest' is typical (the right arrow in Fig. 2a), melanoma has no such topological regularity. Each melanoma has its unique shape, and in the OCT image one can distinguish only the biotissue inhomogeneities. Note, that there are also the basal cell carcinoma neoplasms that have no characteristic shape, but look as chaotically spread regions of inhomogeneity in the healthy biotissue.

The OCT studies of 27 skin neoplasms have shown that the diagnosis of the tumour type based on this method solely is possible only in the case of basal cell carcinoma. Seven of nine studied samples of basal cell carcinoma contained characteristic roundish inhomogeneities, and in two samples it was absent. It follows that the diagnosis of basal cell carci-

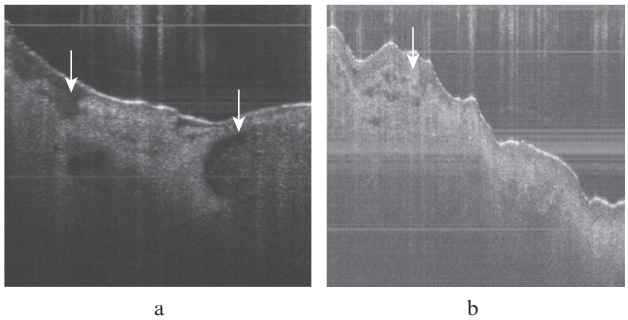

a b

Figure 2. OCT images of (a) basal cell carcinoma and (b) malignant skin melanoma. The size of the studied region is 1.5×1.5 mm. Arrows point at the pathology regions.

noma using OCT allows one to attain ~80% sensitivity. The obtained results agree with those of other studies [15]. The impossibility of determining the tumour type only by means of imaging methods stimulates the use of spectroscopic techniques for this aim.

3.2. Analysis of RS spectra of neoplasms

Relative intensities of RS spectral lines can essentially differ from one studied sample to another. This fact is due to the different concentration of substances in the tissues of different groups of patients. That is why the intensity of all spectra was normalised to the maximal intensity of the peak within the band 1430–1460 cm^{-1}.

The characteristic normalised RS spectra of neoplasms and normal skin are presented in Fig. 3. It is seen that the maximal intensity in the RS spectrum belongs to the band 1430–1460 cm^{-1}, corresponding to the bending vibration mode CH_2/CH_3. Alongside with this band, the bands 1240–1280 cm^{-1} (CN vibration longitudinal mode), 1300–1340 cm^{-1} (bending and twisting modes of CH_2 bond), 1540–1580 cm^{-1} (deformation mode of C=C bond and tryptophan) and 1640–1680 cm^{-1} (C=O longitudinal vibration mode in Amid I compounds) were clearly observed [16].

The most essential changes in the RS spectra of neoplasms in comparison with the RS spectra on normal skin occur in the bands 1300–1340 cm^{-1} and 1640–1680 cm^{-1}. While in the 1640–1680 cm^{-1} band the decrease in the absolute RS intensity is observed for all types of malignant neoplasms, in the 1300–1340 cm^{-1} band, in contrast to the results of Ref. [17], the absolute RS intensity decreases for the basal cell carcinoma and increases for melanoma, as compared to that for the normal skin.

It is also worth noting that, in contrast to Refs [18, 19], in the experiments carried out here the double structure of the RS peak was observed in the region 1300–1340 cm^{-1}. For all types of malignant neoplasms the intensity is redistributed between the two peak components as compared to the RS intensity distribution for normal skin in the considered spectral region (Fig. 3).

The difference between the RS spectra of neoplasms and healthy skin can be related to the increase in the concentration of nucleic acids and the change in the proteins structure [18, 19] in the neoplasm cells, and the change in the absolute RS intensity is possibly explained by the decrease in the density of proteins, embedded in neoplasm cell membranes, and by the increase in the general specific weight of these cells.

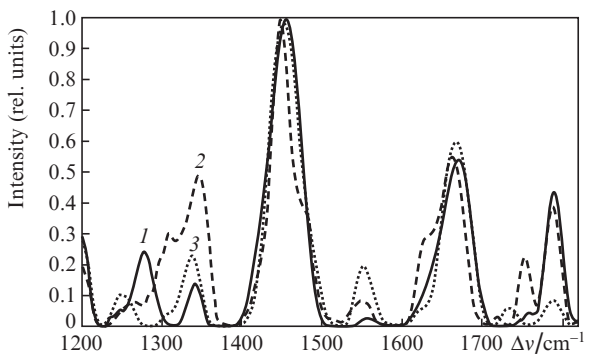

Figure 3. Normalised RS spectra of (*1*) healthy skin, (*2*) melanoma and (*3*) basal cell carcinoma.

The registration of intensities of certain bands in the RS spectrum of a neoplasm allows the determination of its type. In our study the following bands were chosen for this aim: 1300–1340 cm^{-1}, 1440–1480 cm^{-1} and 1640–1680 cm^{-1}.

Most of the known methods for analysing RS spectra of skin neoplasms [16–22] are based on introducing the so-called threshold intensities in the bands 1300–1340 cm^{-1}, 1640–1680 cm^{-1} and 1440–1460 cm^{-1}. In this case the sensitivity and specificity of the methods based on the absolute threshold characteristics do not exceed 78%–82%.

The studies performed by us allow the formulation of a different algorithm for analysing the RS spectrum of neoplasms, namely, the calculation of phase criteria for determining the tumour type. For this goal the phase method of neoplasm analysis is used, which consists in the following.

At the first stage the obtained RS spectra are sequentially analysed. Then two phase characteristics are introduced, I_{1320} and I_{1660}, which are the intensities of the maxima in the bands 1300–1340 cm^{-1} and 1640–1689 cm^{-1} divided by the intensity of the maximum in the band 1440–1460 cm^{-1}. Thus, every measurement can be presented as a point in the phase plane with the coordinates I_{1320} and I_{1660}. Using the histological studies of the samples performed independently of the spectral measurements as a reference method, we can attribute each experimental point in the phase plane to the particular type of a tumour or to healthy tissue.

To assign the classes in the phase plane we used the linear discriminant analysis. The quality of the approach was characterised by its sensitivity and specificity.

3.3. Combined application of OCT and RS spectroscopy for diagnosis of pathologies

Using the OCT and RS methods together, it is rather simple to establish the neoplasm location in healthy tissue. The OCT provides a precise morphological picture of the neoplasm, thus helping a surgeon to determine the invasion zone and to reduce the zone of resection. Figure 4 presents the photograph of a neoplasm in the lung bronchus and its OCT image. The OCT image makes it possible to understand that the pathology is developing in the healthy tissue, but the determination of its type from a B scan is impossible. After detection and delimitation of the tumour one should perform the registration of RS spectra from the regions of pathology and from the normal tissue.

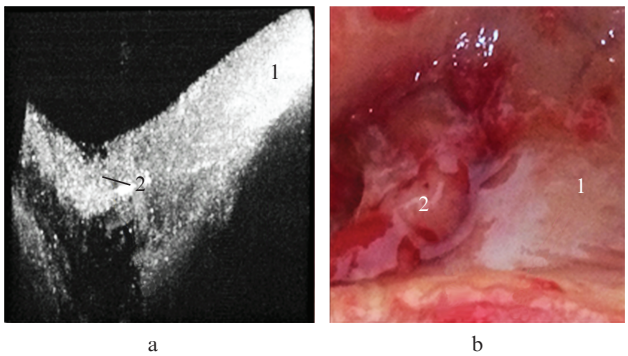

Figure 4. (a) OCT image and (b) digital photograph of the bronchus sample with labels for performing the RS investigation: (*1*) normal biotissue and (*2*) tumour.

At the stage of the analysis of RS spectra the data from the phase planes were used. This allowed successful selection of malignant neoplasms against the background of healthy tissue and identification of skin melanoma. Figure 5 presents the phase plane for the lung investigation. The determination of a malignant neoplasm is possible with high sensitivity and specificity (81% and 84%, respectively), but the identification of a particular type of neoplasm (adenocarcinoma or squamous cell carcinoma) is difficult.

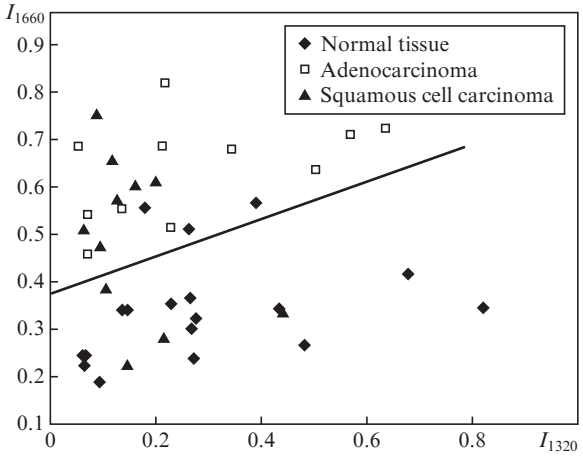

Figure 5. Determination of the lung tissue type in *ex vivo* studies. The straight line separates the phase points, corresponding to the normal tissue and the tissue with neoplasms.

The precalculated values of the sensitivity and specificity of the *ex vivo* melanoma diagnosis using the phase method amounted to 87.5% and 92%, respectively. For *in vivo* studies the sensitivity of melanoma detection was 77.7% and the specificity was 97.8% (Fig. 6).

From the analysis of Figs 5 and 6 it follows that the use of the biotissue RS spectral data allow reliable diagnosis of malignant neoplasms with the sensitivity ~85%.

3.4. Analysis of AF spectra

To increase the informativity of diagnosis in the performed study we used the analysis of the AF spectrum. The AF spectroscopy has been used earlier many times to detect the pathologies of human skin and lungs. It is known that biotissues contain chromophores, such as elastin, collagen, keratin and NADH that contribute to the fluorescence spectrum, as well as purely absorbing chromophores, namely, melanin and haemoglobin. The AF spectroscopy was applied to the diagnosis of various skin neoplasms: the melanocyte-associated ones (melanoma, pigmented nevus), basal cell carcinoma, and squamous cell carcinoma, etc. [23–30], as well as lung malignant tumours [31].

In the present work we performed the AF analysis of skin and lung neoplasms with the AF excited by the radiation with the wavelength 785 nm. The AF spectrum is affected by nucleic acids, fats, melanin, haemoglobin, and proteins, such as elastin, collagen and keratin [32]. The characteristic AF spectrum of skin and lung neoplasms has the form of an exponential function, decreasing with the growth of the wavelength. Typical averaged spectra of neoplasms in the biotissues of the studied samples are presented in Fig. 7. From Fig. 7a it is seen that the

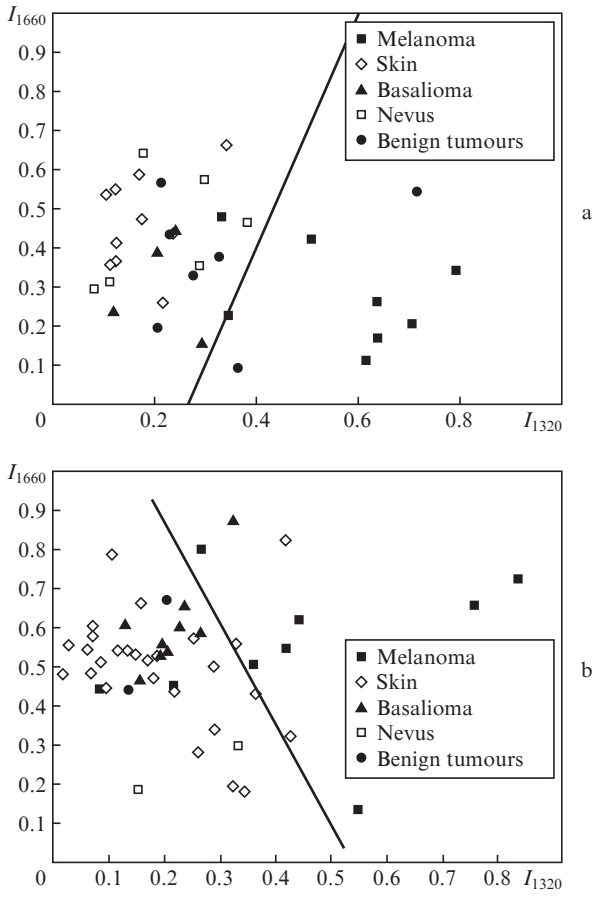

Figure 6. Determination of the skin tissue type in the (a) *ex vivo* and (b) *in vivo* studies. Straight lines separate the phase points, corresponding to normal skin and the skin with neoplasms.

AF intensity of the normal tissue is significantly larger than the AF intensity of the cancer tumour, and from Fig. 7b it follows that the AF intensity of melanoma essentially exceeds the AF intensity of the normal skin, in spite of the considerable spread of intensity values (~40%) in the melanoma spectrum. Such a spread in the intensity values is caused by the permanent decrease in the AF signal value with time during the continuous illumination of the tissue sample with the exciting laser radiation.

Based on the analysis of the obtained spectra of skin neoplasms, we proposed a quantitative criterion for characterising the spectrum shape, approximated by a second-order polynomial, by its curvature in the interval 810–850 nm. Thus, for melanocyte-associated neoplasms a specific 'hump' shape of the spectrum was observed in this interval. The proposed criterion allowed diagnosing nevuses and pigmented melanomas with the accuracy close to 100%; however, the differentiation of pigmented melanomas and nevuses appeared to be practically impossible. Moreover, this criterion of the spectral shape assessment is not efficient for the diagnosis of non-pigmented melanoma.

One of the possible areas of application of the fluorescence analysis is the fast (since the AF signal acquisition time is a few tenths of a second) tumour delimitation without identifying the neoplasm type. Figure 8 presents the intensity of AF from the squamous cell carcinoma in lung tissue and the nevus in healthy tissue, sequentially recorded at the control points of the samples of the studies biotissues at the dis-

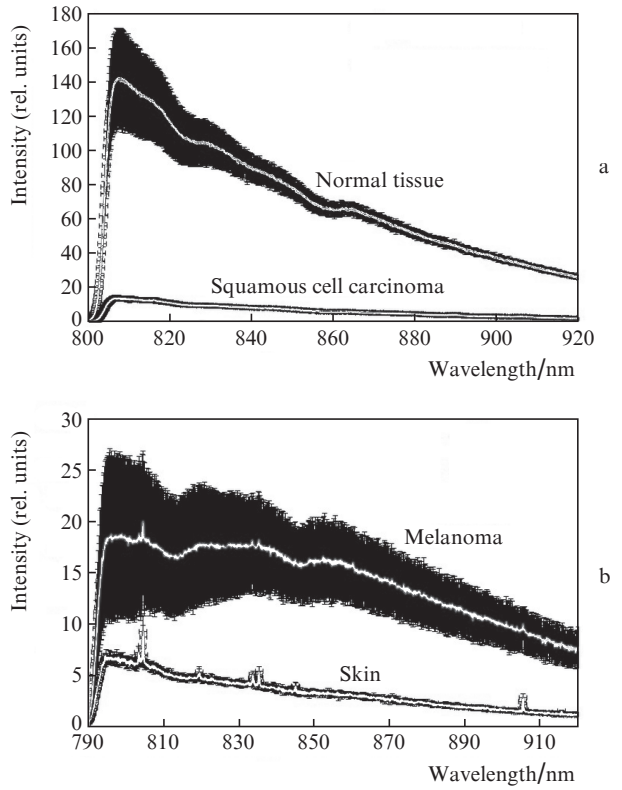

Figure 7. Typical AF spectra of (a) squamous cell carcinoma and (b) melanoma, as well as of healthy tissues of lung and skin, respectively. The confidence intervals are indicated.

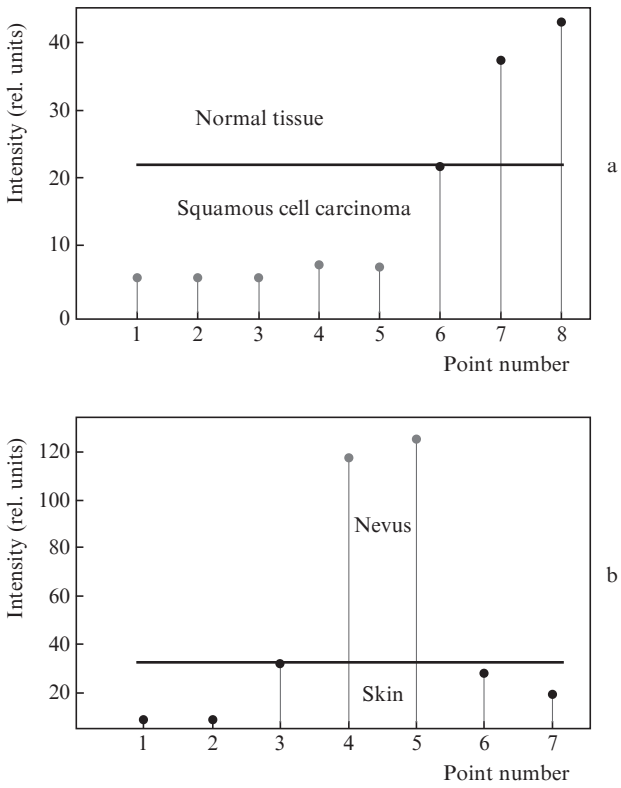

Figure 8. Intensities of AF from squamous cell carcinoma in (a) lung tissue and (b) nevus in skin, sequentially recorded at the control points on the samples, separated by the distance 2.5 mm.

tance of 2.5 mm from each other. The calculation of the threshold AF intensity was implemented using the Otsu method [33]. In Fig. 8a points 1–5 correspond to the tumour, and points 6–8 correspond to healthy lung tissue. These results confirm the above statement that the AF signal for the squamous cell carcinoma is essentially smaller than for healthy tissue.

In Fig. 8b points 4, 5 correspond to the nevus and points 1–3, 6 and 7 to normal skin. These results confirm the possibility of successful application of AF for the tumour delimitation in tissue. The precision of the neoplasm delimitation in this case depends only on the diameter of the laser beam that excites AF of biotissue. In the present paper the laser beam diameter was 1 mm.

The combined use of AF and RS spectroscopy will allow fast detection of the pathology and its delimitation, and, if necessary, also the neoplasm type identification at a particular point, which, in turn, will reduce the time of diagnosis and increase its precision.

4. Conclusions

The first results of studying the resolution power of the combined method, including RS spectroscopy and OCT with the phase analysis of the obtained parameters demonstrate its high efficiency for the diagnosis of lung tumour tissues and skin melanoma. The safety and quickness of the performed examination confirm the high potential of the method. A further increase in the diagnosis precision will require more sophisticated algorithms for analysing the data on the RS spectra of neoplasms.

The efficiency of the neoplasm analysis can be also increased using the data of the biotissue AF. On average, the incorporation of these data increases the precision of neoplasm type identification by 5%–8%. One more advantage of the AF study is the quickness of the performed analysis. The developed experimental setup allows fast scanning of large areas of biotissue using the AF spectroscopy, and the further three-dimensional analysis of suspicious regions aimed at delimiting the pathology should be implemented using the OCT technique, which is more inertial, but provides the micron spatial resolution. The final determination of the tumour type requires the data from the RS spectra of the neoplasm to be taken into account. Each method of diagnosis can be used independently, which allows a surgeon to make use of the advantages of a particular approach with adaptation to a particular patient. The considered combined method may become a powerful tool for an oncologist because of the automatic determination of the tumour type, scanning of organs and high-precision imaging of the neoplasm location in the healthy tissue.

One more advantage of the proposed method is its invariance with respect to the tumour size: the diagnosis precision is not reduced when analysing neoplasms with the diameter smaller than 5 mm, while in visual examination by a surgeon the small size of a neoplasm essentially complicates the diagnosis and its efficiency is reduced to 40%.

Acknowledgements. The work was supported by the Ministry of Education and Science of the Russian Federation.

References

1. Mathers C.D., Loncar D. *PLoS Med.*, **3**, 2011 (2006).

2. Boyle P., Levin B., in *World Cancer Report 2008* (Lyon: IARC Press, 2008).
3. Ferlay J., Bray F., Pisani P., in *Cancer Incidence in Five Continents* (Lyon: IARC Press, 2004).
4. Friedman R. *Arch. Dermatol*., **4**, 554 (2008).
5. Mogensen M., Thrane L., Jorgensen T.M., Andersen P.E., Jemec G.B.E. *J. Biophoton*., **2**, 442 (2009).
6. Myakinin O.O., Kornilin D.V., Bratchenko I.A., Zakharov V.P., Khramov A.G. *J. Innov. Opt. Heal. Sci*., **6**, 19 (2013).
7. Mogensen M., Nürnberg B.M., Forman J.L., Thomsen J.B., Thrane L., Jemec G.B.E. *British J. Dermatol.*, **160**, 1026 (2009).
8. Zakharov V.P., Larin K., Bratchenko I.A. *Vestnik Samarskogo Gos. Aerokosm. Univer*., **26**, 232 (2011).
9. Huang Z., McWilliams A., Lui H., David I., McLean D.I. *Int. J. Cancer*, **107**, 1047 (2003).
10. Haka A.S., Shenk R., Dasari R.R., et al. *J. Biomed. Opt*., **14**, 054023 (2009).
11. Mavarani L., Petersen D., El-Mashtoly S.F., Mosig A., Tannapfel A., Kötting C., Gerwert K. *Analyst*, **138**, 4035 (2013).
12. Zakharov V.P., Bratchenko I.A., Artemyev D.N., Myakinin O.O., Larin K.V., Kozlov S.V., Moryatov A.A., Khristoforova Yu.A. *Fiz. Voln. Prots. Radiotekh. Sistemy*, **16**, 73 (2013).
13. Zakharov V.P., Bratchenko I.A., Khristoforova Yu.A. Kornilin D.V. *Opt. Spektrosk*., **115**, 179 (2013) [*Opt. Spectrosc*., **115**, 182 (2013)].
14. Zhao J., Lui H., McLean D.I., Zeng H. *Cancer Res*., **72**, 2492 (2012).
15. Forsea A. *J. Med. Life*, **3**, 381 (2010).
16. Zhao J., Lui H., McLean D.I., Zeng H. *New Develop. Biomed. Eng.*, **24**, 455 (2010).
17. Manoharan R., Wang Y., Dasari R.P., Singer S.S., Rava R.P., Feld M.S. *Laser Life Sci*., **6**, 1 (1995).
18. Vargis E., Mahadevan-Jansen A., in *Using Raman Spectroscopy to Detect Malignant Changes in vivo* (Princeton: Princeton Instruments, 2011).
19. Martin A., Carter R.A., Oliveira Nunes L., Arisawa E.L., Junior L.S. *Biomedical Vibrational Spectroscopy/Biohazard Detection Technologies* (Bellingham, WA: SPIE, 2004).
20. Hanlon E.B., Manoharan R., Koo T.W., Shafer K.E., Motz J.T., Fitzmaurice M., Kramer J.R., Itzkan I., Dasari R.R., Feld M.S. *Phys. Med. Biol*., **45**, R1 (2000).
21. Gniadecka M., Philipsen P.A., Sigurdsson S., Wessel S., Nielsen O.F., Christensen D.H., Hercogova J., Rossen K., Thomsen H.K., Gniadecki R., Hansen L.K., Wulf H.C. *J. Invest. Dermatol*., **122**, 443 (2004).
22. Mogensen M., Jemec G.B. *Dermatol. Surg*., **33**, 1158 (2007).
23. Sterenborg H.J.C.M., Motamedi M., Wagner R.F., Thomsen S., Jacques S.L. *Proc. SPIE Int. Soc. Opt. Eng.*, **2324**, 32 (1994).
24. Sterenborg H.J.C.M., Motamedi M., Wagner R.F., Duvic M., Thomsen S., Jacques S.L. *Laser. Med. Sci.*, **9**, 191 (1994).
25. Andersson-Engels S., Canti G., Cubeddu R., Eker C., af Klinteberg C., Pifferi A., Svanberg K., Svanberg S., Taroni P., Valentini G., Wang I. *Laser. Med. Sci.*, **26**, 76 (2000).
26. Borisova E.G., Troyanova P.P., Stoyanova V.P., Avramov L.A. *Proc. SPIE Int. Soc. Opt. Eng.*, **5830**, 399 (2005).
27. Borisova E., Dogandjiiska D., Bliznakova I., Avramov L., Pavlova E., Troyanova P. *Proc. SPIE Int. Soc. Opt. Eng.*, **7368**, 24 (2009).
28. Borisova E., Troyanova P., Pavlova P., Avramov L. *Kvantovaya Elektron*., **38**, 597 (2008) [*Quantum Electron*., **38**, 597 (2008)].
29. Wang S., Zhao J., Lui H., He Q., Zeng H. *Skin. Res. Technol*., **19**, 20 (2013).
30. Lauridsen R.K., Everland H., Nielsen L.F., Engelsen S.B., Nørgaard L. *Skin. Res. Technol.*, **9**, 137 (2003).
31. Al-Salhi M., Masilamani V., Vijmasi T., Al-Nachawati H., Vijaya-Raghavan A.P. *J. Fluoresc*., **21**, 637 (2011).
32. Bigio I.J., Mourant J.R., in *Encyclopedia of Optical Engineering* (New York: Marcel Dekker, 2003).
33. Otsu N. *IEEE Trans. Syst. Man Cybern.*, **9**, 62 (1979).